Journal of Catalysis 268 (2009) 367–375

Contents lists available at ScienceDirect

Journal of Catalysis

journal homepage: www.elsevier.com/locate/jcat

CO-TPR-DRIFTS-MS *in situ* study of $CuO/Ce_{1-x}Tb_xO_{2-y}$ ($x = 0$, 0.2 and 0.5) catalysts: Support effects on redox properties and CO oxidation catalysis

Aitor Hornés [a], Parthasarathi Bera [a], Antonio López Cámara [a], Daniel Gamarra [a], Guillermo Munuera [b], Arturo Martínez-Arias [a,*]

[a] Instituto de Catálisis y Petroleoquímica, CSIC, C/Marie Curie 2, Campus de Cantoblanco, 28049 Madrid, Spain
[b] Departamento de Química Inorgánica e Instituto de Ciencia de Materiales (Centro Mixto Universidad de Sevilla–CSIC), 41092 Sevilla, Spain

ARTICLE INFO

Article history:
Received 6 August 2009
Revised 5 October 2009
Accepted 6 October 2009
Available online 3 November 2009

Keywords:
CuO catalysts
CeO_2
Ce–Tb mixed oxides
CO-TPR
DRIFTS
XPS
CO-PROX

ABSTRACT

Catalysts of copper oxide supported on CeO_2 and $Ce_{1-x}Tb_xO_{2-y}$ have been studied by temperature-programmed reduction employing CO as a reductant (CO-TPR) using a diffuse reflectance infrared Fourier transform spectroscopy (DRIFTS) cell as well as conventional tubular reactors in order to get insights into redox changes occurring in the course of interaction of the systems with CO. CO-TPR results collected in the classical way, i.e. starting the temperature ramp after reactant gas equilibration at room temperature, suggest that the reduction of the copper species occurs at temperatures which decrease with the terbium content of the support. However, such result contrasts with CO oxidation activity of the systems under CO-PROX condition which follows just the opposite trend. DRIFTS results and analysis of low temperature redox processes, typically disregarded during recording of classical TPR tests, show that catalytic activity can be correlated to the magnitude of reduction achieved already at room temperature, which is related to reduction of interfacial copper oxide species.

1. Introduction

CO abatement reactions such as water gas shift (WGS), preferential oxidation of CO in H_2-rich streams (CO-PROX) or its simple oxidation either with O_2 or NO have been paid much attention since CO is an atmospheric pollutant and a poison for fuel cells [1–9]. In particular, for processes involving CO oxidation, catalysts based on closely interacting CuO and CeO_2 have shown outstanding performances, comparable to those exhibited by less economically interesting precious metal catalysts [7,9,10]. The ability of copper oxide-ceria catalysts for such reaction has been related to the promotion of redox properties which is achieved upon combination of both oxides, taking into account that they apparently operate under a redox-type catalytic mechanism [7,11]. The redox promotion has been mainly based on intensive investigation done with different spectroscopic techniques as well as temperature-programmed reduction (TPR) studies in which it has generally been shown that the CO oxidation rate can be correlated with the ceria-promoted reducibility attained on the disperse copper oxide entities [7,9,12–16]. In turn, the degree of promotion of such reduction can be also affected by modifying the nature of the support within structurally related doped ceria materials [8,17].

Recent work by Luo et al. provides an important rationalization of redox/catalytic correlations in catalysts combining copper and cerium oxides on the basis of CO-TPR results [18]. Thus, they differentiate between the reducibilities of the three types of oxidized copper entities generically proposed to be present in this type of catalysts, in agreement also with previous investigation [12,13]: in decreasing order of reducibility, finely dispersed CuO, bulk-like CuO and Cu^{2+} incorporated, likely substitutionally [19], to the ceria lattice. Furthermore, they propose the possibility to estimate quantitatively the relative contribution of each of these oxidized copper entities to the overall CO oxidation activity [18]. Nevertheless, such investigation has been done on a series of catalysts combining in all cases copper oxide (as supported component) and ceria (as support) while, as mentioned, changes in the support nature can modify such redox or catalytic properties [8,17]. This can be attributed to differences in the respective copper oxide-support interfacial properties, whose specific characteristics have recently been shown to be most relevant to explain CO oxidation catalytic properties [7].

Within this context, in the present contribution we propose a study of a series of $CuO/Ce_{1-x}Tb_xO_{2-y}$ catalysts with the same copper loading but differing in the support composition (x between 0 and 0.5) mainly by employing CO-TPR tests with mass spectrometry detection. In order to get information for redox changes taking place during the course of such tests, parallel experiments have been performed for which a DRIFTS cell has been used as a reactor

* Corresponding author. Fax: +34 91 585 4760.
E-mail address: amartinez@icp.csic.es (A. Martínez-Arias).

0021-9517/$ - see front matter © 2009 Elsevier Inc. All rights reserved.
doi:10.1016/j.jcat.2009.10.007

and the corresponding spectra have been simultaneously recorded. For the sake of completeness, the corresponding supports employed as references have also been explored by the same techniques. As a complementary basis, results of characterization at structural and electronic levels of the catalysts employed as well as catalytic properties for the CO-PROX process are available in previous works of the group [8,9], while additional XPS experiments are presented in order to complement the redox analysis. The present work will show that correlation between redox and catalytic properties in reactions involving CO in this type of catalysts requires, in agreement with recent work [7], a detailed analysis of interfacial redox properties, not necessarily directly provided by classical TPR profiles (i.e., starting after equilibration of the reactant gases at the lowest possible temperature, in our case as in most studies, room temperature).

2. Experimental

The $Ce_{1-x}Tb_xO_{2-y}$ supports were prepared by reverse microemulsion method. For this, aqueous solutions of corresponding nitrate salt precursors of Ce or Ce and Tb (at nominal atomic ratios of Ce/Tb = 1 and 4) were introduced in a reverse microemulsion (water in oil) using *n*-heptane (Scharlau) as the organic phase, Triton X-100 (Aldrich) as the surfactant and 1-hexanol (Aldrich) as the co-surfactant. Then this microemulsion was mixed with another one of similar characteristics containing dissolved tetramethylammonium hydroxide (TMAH, Aldrich) in its aqueous phase in order to coprecipitate the cations. The resulting mixture was stirred for 24 h followed by centrifugation, decanting and rinsing of the resulting solid with methanol. Finally, the solid portion was dried at 110 °C for 24 h and the resulting powders were calcined under air at 500 °C for 2 h. Details of the preparation parameters employed during the synthesis of these supports can be found elsewhere [20,21]. Chemical analysis by ICP-AES showed Ce/Tb atomic ratios of 1.1 and 3.93, respectively, indicating that within experimental error quantitative precipitation of both Ce and Tb cations was achieved. CeO_2 and CuO references were prepared following the same procedure. The copper oxide catalysts supported on the corresponding CeO_2 and Ce–Tb mixed oxides were prepared by incipient wetness impregnation of the corresponding support using aqueous solutions of $Cu(NO_3)_2{\cdot}3H_2O$ to get a final copper loading of 1 wt.% in all cases. The resulting material was dried overnight at 110 °C and subsequently calcined under air at 500 °C for 2 h. The nomenclature used for these catalysts as well as their main textural or compositional properties is summarized in Table 1.

Temperature-programmed reduction experiments employing CO as a reductant (CO-TPR) were carried out by employing a Pfeiffer Omnistar mass spectrometer (MS) as a detector. Either a simple quartz tube or a diffuse reflectance infrared Fourier transform spectroscopy (DRIFTS) cell (Harrick), fitted with CaF_2 windows and a heating cartridge that allowed samples to be heated to 500 °C, was employed as a reactor. Prior to the CO-TPR run, the samples were calcined *in situ* at 500 °C under a flow of 20% O_2/He for 2 h. Then, after cooling to room temperature under that oxidizing atmosphere and extensively purging under inert gas, the sample was exposed to 5% CO/He flow at room temperature until gas equilibration. Then, when the concentrations of all monitored gases became constant, the sample temperature was raised under the diluted CO atmosphere using a ramp of 10 °C min^{-1} and a flow of 500 cm^3 min^{-1} g^{-1} in any of the two reactors (500 and 100 mg of catalyst being employed for the tests in the tubular and DRIFTS cell reactors, respectively). *Operando* DRIFTS analysis of the samples was carried out using a Bruker Equinox 55 FTIR spectrometer fitted with an MCT detector. The spectra (average of 20 scans at 4 cm^{-1} resolution) were recorded typically at every 10 °C. For comparison with the spectra of gaseous CO molecules whose shape changes with the temperature as a consequence of differences in populations of rotational levels, blank runs were done under the same conditions with KBr. All the DRIFTS data presented have accordingly been subtracted from the corresponding CO(g) data at each temperature in order to get rid of contribution from CO(g). All the gases employed were supplied by Air Liquide and had purity higher than 99.95%.

X-ray photoelectron spectra (XPS) were recorded with a Leybold–Heraeus spectrometer equipped with an EA-200 hemispherical electron multichannel analyser (from Specs) and a 120 W, 30 mA Al Kα X-ray source. The sample (ca. 0.2 g) was slightly pressed into a small (4 × 4 mm) pellet and then mounted on a sample rod and introduced into the pretreatment chamber where it was outgassed at 200 °C for 2–3 h, until a pressure of less than 2.0×10^{-8} Torr was achieved; thermal treatments under CO or O_2 (ca. 1 Torr), followed by outgassing, were carried out in the same pretreatment chamber as required. The spectrum intensities were estimated by calculating the integral of each peak after subtraction of an S-shaped Shirley type background with the help of UNIFIT for Windows (Version 3.2) software; atomic ratios were then derived using the appropriate experimental sensitivity factors. All binding energies (BE) were referenced to the adventitious C1s line at 284.6 eV. This reference gave BE values with an accuracy of ±0.1 eV; the peak u''' characteristic of Ce^{4+} was thus obtained at 917.0 ± 0.1 eV. In the case of the Ce3d or Tb3d spectra, factor analysis (also known as principal component analysis) was used to calculate the Ce^{3+}/Ce^{4+} or Tb^{3+}/Tb^{4+} ratios in each set of spectra recorded, using the methodology developed in previous works [22,23].

3. Results and discussion

Characterization: Details about characterization of these catalysts have been reported in our earlier publications [8,21,23]. For the sake of completeness, a brief account of such results is given hereafter. Concerning bulk structural characteristics and on the basis of XRD, HREM and Raman, the catalysts are constituted by aggregates of variable size in the range of 0.1–1.0 μm which are formed by nanocrystals of ca. 5.5–8.5 nm size with the fluorite structure (Table 1); no hint of copper-containing phases could be detected by any of these techniques, thus indicating a relatively

Table 1
Summary of basic physico-chemical properties for the indicated catalysts; cell parameters and crystal size correspond to the fluorite phase of the support, only one detected by XRD due to the relatively large copper dispersion and considering also its relatively low loading [8,21].

Catalysts	Composition	S_{BET} (m^2 g^{-1})	Cell parameter (Å)	Crystal size (nm)
CuCe	1% Cu/CeO_2	107	5.413	8.3
CuCeTb4	1% $Cu/Ce_{0.8}Tb_{0.2}O_{2-x}$	105	5.393	7.2
CuCeTb1	1% $Cu/Ce_{0.5}Tb_{0.5}O_{2-x}$	100	5.368	6.1
CeO_2	CeO_2	130	5.412	7.7
CeTb4	$Ce_{0.8}Tb_{0.2}O_{2-x}$	104	5.401	6.6
CeTb1	$Ce_{0.5}Tb_{0.5}O_{2-x}$	95	5.368	5.5

high dispersion degree for such entities. Analysis of lattice parameters of the nanocrystals reveals, in agreement with XPS and XANES analysis [23], the presence of variable amounts of Tb^{3+} and Tb^{4+} as a function of the terbium content: ca. 62% and 46% of the terbium appears as Tb^{3+} in CeTb4 and CeTb1 according to such estimation (and the same in the corresponding copper-containing catalysts, according to the absence of important XRD differences, Table 1); in turn, cerium appears in all cases in a fully oxidized Ce^{4+} state according to XPS and XANES [8,9,12,23]. Thus, in accordance with these results and despite the stabilization of higher amounts of Tb^{4+} with increasing the amount of terbium, it can be noted that the absolute amount of oxygen vacancies increases with increasing the terbium content, in agreement with Raman investigation [21], as well as with previous results by other authors [24].

Concerning characterization of the copper, XANES or XPS results (as also described below) have shown that it presents a fully oxidized state (Cu^{2+}) in all the initial samples (after calcination under diluted oxygen) and appears essentially in the form of highly dispersed CuO-type species [8,9]. Further details were achieved by EPR on the CuCe sample although such analysis could not unfortunately be extended to the terbium-containing samples due to the presence of strong magnetic interactions with Tb^{3+} and/or Tb^{4+}, both being paramagnetic. The presence of ca. 35% of the copper in the form of small, highly dispersed copper oxide clusters was inferred from such EPR results on CuCe while a residual amount of isolated Cu^{2+} species was also detected; the rest of the copper was EPR-silent, which was attributed to antiferromagnetic interactions between the Cu^{2+} cations into less dispersed (even though still undetectable by XRD) CuO particles [12]. This interpretation was also in agreement with Ar^+-sputtering XPS results [12].

CO-TPR MS analysis with the tubular reactor: The evolution of CO_2 during CO-TPR runs performed with the tubular reactor over the different samples, commencing the recording after a period of gas equilibration at room temperature, is shown in Fig. 1. The TPR profile of pure CuO is also included in the same figure for comparative purpose. This profile reveals that the CO reduction on pure CuO starts at ca. 150 °C and displays a broad and asymmetric peak centred at 295 °C which, considering the conditions employed, can be assigned to direct reduction to metallic copper, in agreement with previous studies [25]. It may be noted that the reduction temperature appears somewhat lower than that observed during CO-TPR or related analyses on other CuO samples by other authors [25,26], which can be related to the lower size particles, likely more easily reducible [27], present in our case. It may be also noted that the CO-TPR profile (as it occurs also for the other copper-containing catalysts) does not return back completely to the baseline although the maximum reduction level attained appears far from the final temperature employed. This has been commonly observed for other supported copper catalysts [18,28,29], and apparently contrasts with the behaviour observed during similar runs when H_2 was employed as a reductant [30–32]. This can be related to occurrence of the Boudouard reaction ($2CO \rightarrow C + CO_2$) which can be promoted at high temperature in the presence of metallic copper [33,34]; alternatively, an experimental artefact related to possible chemisorption and slow desorption of CO_2 in the MS detection system has been also pointed out [25]. However, recent investigation done on the CuCe catalyst by comparing ^{12}CO- and ^{13}CO-TPR experiments, subsequently followed by TPO tests, has allowed to conclude that no carbon deposits are formed in the sample treated under CO up to 400 °C and that the process responsible for the residual CO_2 amount detected at 400 °C in the CO-TPR profile must be mainly related to the remaining WGS processes resulting from CO interaction with surface hydroxyl species [35], in agreement also with recent investigation by Caputo et al. [36].

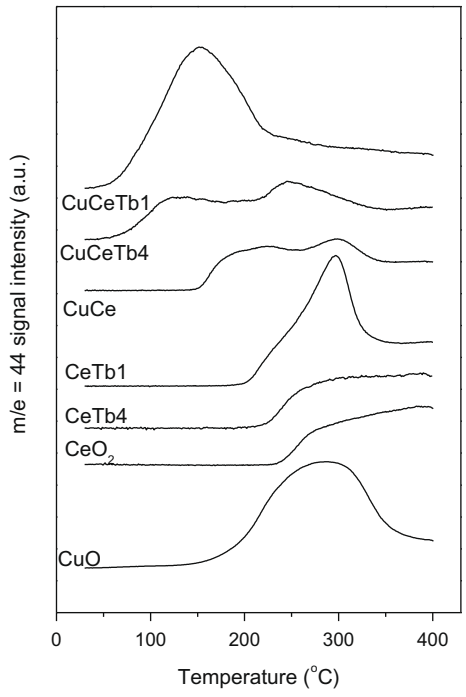

Fig. 1. CO_2 production during the CO-TPR runs performed with the tubular reactor over the indicated samples.

Concerning the CeO_2 support, the reduction starts around 250 °C and does not appear to have completed at the end of the run at 400 °C, in good agreement with the literature results [37,38]. In the presence of 20% Tb (CeTb4) a downward shift of the reduction onset to 215 °C and a somewhat higher overall level of reduction appear to be attained within the examined range. In turn, in the case of CeTb1 support, reduction starts at 200 °C and a sharp intense peak at 298 °C and a shoulder peak at 225 °C are apparent while overall reduction level increases appreciably. These results demonstrate that low temperature reducibility of CeO_2 under CO is improved in the presence of Tb and that the reducibility of the mixed oxide increases with the amount of Tb. Results in the same sense were observed in a study of the reducibility of materials of this type under hydrogen [39].

The reduction profile of CuCe is characterized by a low intensity reduction peak and a somewhat stronger peak at about 170 and 225 °C, respectively, which are referred to as α and β peaks, according to the usual nomenclature employed in the literature [18]. In addition, there is a high intensity peak at 298 °C (γ peak). These peaks below 300 °C have been assigned to the reduction of Cu^{2+} ions belonging to different types of oxidized copper entities with differing degrees of interaction with the underlying ceria support [18]. In this sense, the presence of more than one reduction peak in CuCe catalyst instead of basically one peak in the case of pure CuO is consistent with the existence of more than one type of copper oxide species in 1CuCe, in agreement with characterization results described above. The reduction of copper species responsible for α and β peaks occurs at lower temperatures compared to that of pure CuO while the γ peak maximum appears fairly close to that of bulk CuO. This justifies attribution of the former two peaks to well-dispersed copper oxide species whose reduction would be appreciably promoted by ceria while the latter accounts for the presence of less dispersed (even though still diffraction silent) copper oxide entities. Comparing with literature results, it must be taken into account that the TPR peak shape and position can strongly depend on the experimental conditions employed and particular copper oxide configurations present in each case. Luo and coworkers have reported three types of CuO species in their CO-TPR analysis of

copper oxide-ceria catalysts prepared by sol–gel or surfactant-templated methods [18,31]; such synthesis methods, as it occurs also for microemulsion-coprecipitation [9,19], may favour introduction of part of the copper into the ceria fluorite structure, in contrast to impregnation method by which most of the copper appears surface dispersed [12]. They detect peak α at ca. 125 °C and attribute it to the reduction of finely dispersed CuO; peak β appearing at ca. 175 °C is attributed to the reduction of Cu^{2+} in the CeO_2 lattice while peak γ at ca. 200 °C is attributed to the reduction of bulk CuO [18,31]. In similar terms, Papavasiliou et al. regard the low temperature features between 70 and 200 °C as the reduction of copper species strongly interacting with CeO_2 and a high temperature maximum between 240 and 270 °C as the reduction of larger copper oxide particles less affected by interaction with the CeO_2 support [29]. Similar attributions of reduction peaks have been reported in the literature on the basis of CO- or H_2-TPR results over catalysts of this type [13,30,40–44].

Apparent downward shifts of the reduction of copper species are observed in the presence of Tb in the support. Thus, the reduction profile of CuCeTb4 contains a low temperature peak at 120 °C whereas two peaks appear at higher temperature (190 and 250 °C). The presence of multiple peaks must reflect, as in the case of CuCe, the heterogeneity of copper oxide entities in this sample. In the case of CuCeTb1, the reduction starts around 50 °C and an intense peak at 155 °C is observed. There is also a hump at 250 °C in this case. Results in the same sense can be found in reports by Wang et al., in which the formation of a low temperature α peak in the case of CuO on samarium-doped ceria has been attributed to the effect of the presence of surface oxygen vacancies within the oxygen ion conducting support [26,45,46]. They have inferred that an interfacial metal oxide-support interaction mechanism is involved at the inception of the reduction, followed by the induced successive reduction of bulk copper oxides. Similarly, our CO-TPR results suggest that the reducibility of finely dispersed CuO on CuCeTb4 and CuCeTb1 can be enhanced in comparison to that on CuCe.

It must be noted that attribution of the CO-TPR features exclusively to reduction of the supported copper oxide entities, as typically done in the mentioned literature, is ignoring the fact that the reducible supports can also be involved in the reduction processes. This has been demonstrated previously on the basis of not only spectroscopic proof [2,6,12,17], but also quantitative TPR [30,32,36,47]. Indeed, quantification of the overall CO_2 produced during the tests displayed in Fig. 1 for CuCe, CuCeTb4 and CuCeTb1 yields values of ca. 605, 506 and 812 μmol g^{-1}, respectively, largely exceeding the CO_2 production expected for exclusive reduction of copper oxide entities (such values correspond to between ca. 3.2 and 5.2 CO molecules consumed per copper atom). Involvement of the supports in the reduction processes is also supported by XPS, as will be described later. Specific experiments would be however required to determine the respective contributions of the supports (and, furthermore, of cerium or terbium components in them) to the different features present in the CO-TPR profiles while the analysis is further complicated by the possible existence of different reduction processes involving not only oxide but also hydroxyl species [35,36].

Correlation with catalysis for CO oxidation: In any case, the apparently enhanced reduction of dispersed copper oxide entities detected upon Tb-doping of ceria in the CO-TPR profiles of Fig. 1 does not correlate with gradual decrease in CO oxidation activity under CO-PROX conditions observed by increasing the amount of Tb for these catalysts [8]. It has to be noted that such type of redox/catalytic correlations appear well established on the basis of both CO-TPR and H_2-TPR experiments [13,18,30,31]. However, these studies involve systems which differ in the nature (or dispersion degree) of the supported copper oxide entities and not in the nature of the support. The results reported here evidence that such type of correlation is not fully valid when the nature of the support changes, at least for Ce–Tb mixed oxides as examined here; note in this sense that such correlations might still be valid when comparing pure ceria and Ce–Zr mixed oxide supported catalysts [5,47,48]. In any case, what could be the reason for the discrepancies encountered when using $Ce_{1-x}Tb_xO_{2-y}$-supported systems, taking also into account that correlation between copper oxide reducibility and CO oxidation activity has been demonstrated not only with the mentioned TPR experiments but also on the basis of various spectroscopic techniques [7]? The origin of the discrepancy can be related to the redox phenomena taking place at relatively low temperature (even sub-ambient), in this case during the gas equilibration period carried out at room temperature before starting the TPR test with the heating ramp under diluted CO. Indeed, a process of CO consumption, with no CO_2 evolution, is detected during such equilibration period, in agreement also with recent results [35,36]. According to the results presented in Fig. 2, the amounts of CO consumed at 20 °C prior to launching the ramp are estimated as 230, 210 and 175 μmol g^{-1} for CuCe, CuCeTb4 and CuCeTb1 samples, respectively. These correspond to about 1.43, 1.30 and 1.08 CO molecules consumed per copper atom, indicating that CO uptake by the support must also take place. Nevertheless, such support consumption appears strongly promoted by the presence of copper, considering that only about 6 μmol g^{-1} is consumed by the CeO_2 support under the same conditions, as supported by the practical absence of the formation of carbonyls or carbonates in the infrared spectra [35]; similarly, practically no change has been detected in the infrared spectrum of the CeTb1 support upon interaction with CO at 20 °C (not shown), thus confirming the copper-promoting effect on support CO uptake also for this system. Similar low temperature redox phenomena in ceria-supported copper oxide catalysts have been recently reported by Caputo et al. on the basis of TPR tests [36]. They are also consistent with the appreciable degree of copper and support reduction observed in previous works by EPR, XPS or Raman upon interaction of the CuCe catalyst with CO, and also with H_2, at room temperature [6,9,12,49,50]. In any case, the respective level of CO consumption at room temperature correlates well, at least qualitatively, with the mentioned results of CO oxidation activity. It therefore appears that main redox phenomena which could correlate with CO oxidation activity in catalysts based on combinations between copper oxide and ceria (or isostructural doped ceria systems) can be those taking place

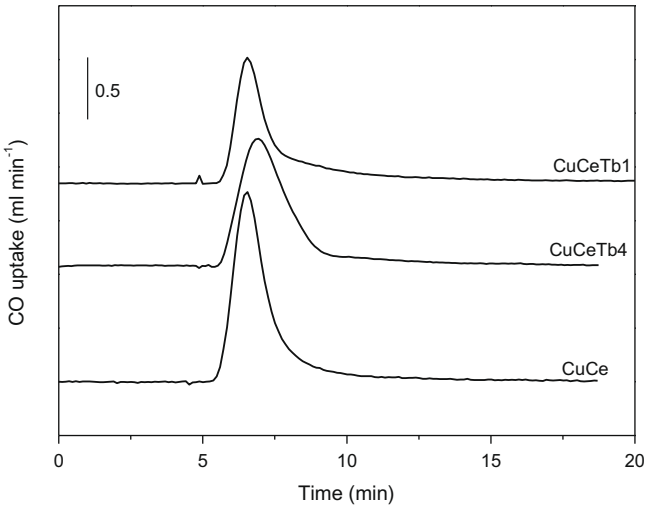

Fig. 2. CO uptake at room temperature during the gas equilibration period prior to launching the CO-TPR heating ramp over the indicated catalysts. Subtraction from a blank experiment employing inert KBr was performed to get the profiles.

at relatively low temperature (typically room or even sub-ambient temperature). This agrees well with results from our group showing that sites active for CO oxidation are related to Cu^+ centres already formed upon reduction at room temperature, which are located at the interfaces between the dispersed copper oxide entities and the support [7]; in the same terms, recent results by other authors have also confirmed the involvement of such type of sites on the reaction [51]. Then, features detected in classical TPR profiles starting after gas equilibration at room temperature (as in Fig. 1) must be related not to the first interfacial reduction but to the propagation of the copper oxide and support reduction to sites not strictly located at interfacial positions, in agreement with our model of redox properties for this type of catalysts [12]. Such extension of the copper oxide reduction to non-interfacial sites has been proposed to provide centres active for H_2 oxidation under CO-PROX conditions [7]. In this sense, the higher facility for such non-interfacial reduction with increasing the Tb content of the support (Fig. 1) is also in agreement with the associated decrease in CO_2 selectivity observed during CO-PROX over these catalysts [8].

CO-TPR-DRIFTS-MS and XPS analyses: In order to get hints on the mentioned low temperature redox phenomena, as well as on those taking place at higher temperature during the CO-TPR tests, these have been additionally performed by employing the DRIFTS cell as a reactor while the corresponding spectra were simultaneously recorded during the course of the run. Fig. 3 displays the evolution of CO_2 during these runs. Some differences are apparent between these profiles and those recorded upon employment of the tubular reactor (Fig. 1). These must be mainly attributed to differences in reactor configurations, as also pointed out previously for other reactions [2,9]. Nevertheless, it can be observed that, as it occurs for runs done with the tubular reactor, the presence of Tb apparently promotes copper oxide reduction also under these conditions according to the profiles of Fig. 3 (note that these are also taken in the classical way, i.e. starting the recording just after launching the heating ramp following achievement of gas equilibration at room temperature).

DRIFTS spectra recorded for the Cu-containing samples during these tests are shown in Figs. 4–6. Bands are observed to be basically formed in two spectral zones generally related to the formation of carbonyl species (stretching region at 2200–2000 cm^{-1}) and carbonate, carboxylate or formate species (most intense modes in 1700–1100 cm^{-1} region), respectively; smaller changes related to

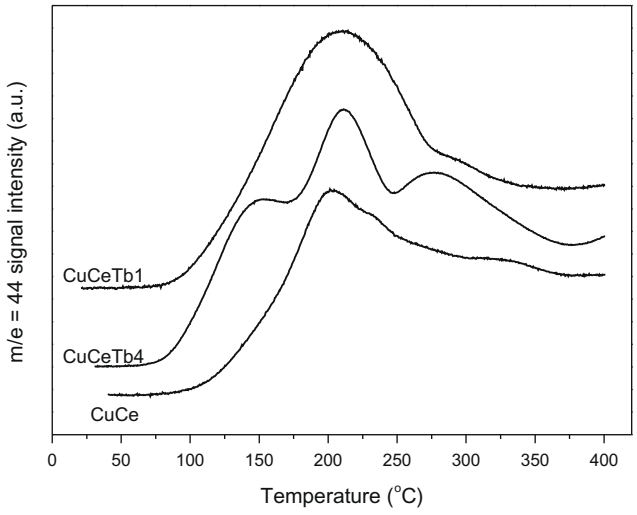

Fig. 3. CO_2 production during the CO-TPR runs performed with the DRIFTS cell reactor over the indicated samples.

reorganization of hydroxyl groups, basically from isolated to associated species by increasing the temperature, during the course of the TPR run, as well as a general decrease of the bands above ca. 300 °C, are also detected in the 3800–3000 cm^{-1} zone (not shown). Main spectral characteristics of the species detected are collected in Table 2. Spectra for the initial calcined samples, prior to contact with CO, display bands in the 1550–1200 cm^{-1} range attributable to carbonate species of bidentate or monodentate type or formate species [52–55]. It must be noted that due to the basic character of ceria, such carbonate-type species are difficult to be eliminated by the oxidizing thermal treatment, typically requiring temperatures above 750 °C, which can induce an important sample sintering and surface area loss [56]. New carbonate-type species, all of them formed over the support part of the catalyst in accordance with previous works of CO or CO_2 chemisorption over CeO_2 [53], are generated upon interaction of the sample with CO. Thus, bi- and mono- or poly-dentate carbonates, as well as, in the case of CuCe, hydrogen-carbonate species are created upon first low temperature contact with CO (Table 2). In turn, formate species are formed at higher temperature.

Concerning the 2400–1800 cm^{-1} region of the spectra, in which carbonyl stretching vibration is expected, two main contributions (apart from the two rotational branches, centred at ca. 2350 cm^{-1}, corresponding to $CO_2(g)$) are apparent. First, a band at ca. 2176–2167 cm^{-1} is attributable to CO adsorbed on unsaturated Ce^{4+} cations (similar carbonyls are the only ones detected when performing the CO-TPR run over the copper-free supports; results for the CeO_2 sample are available elsewhere [35]). Second, a band at 2123–2109 cm^{-1} is formed already upon first contact of the copper-containing samples with CO at room temperature and can be ascribed to Cu^+-carbonyl species in accordance with previous works [9,12,17,49] and as recently confirmed by experiments comparing ^{12}CO vs. ^{13}CO chemisorption over CuCe [35]. This band appears slightly shifted to higher wavenumber in the presence of Tb in the support, suggesting a certain decrease of support influence on its red shift; i.e. π-back-bond component responsible for the red shift, within the usual σ bond-π-back-bond scheme employed to explain carbonyl bonds in this type of species [57,58], would be more hindered in the presence of Tb in the support.

Evolution of the intensity of this Cu^+-carbonyl with temperature during the CO-TPR runs is displayed in Fig. 7. The fact that carbonyls and carbonate-type species are formed already upon first contact of the samples with CO at room temperature is in good agreement with the mentioned CO consumption phenomena produced during gas equilibration prior to starting the heating ramp. Simple chemisorption on the copper oxide component, giving rise to Cu^+-carbonyl species, would take place if such component is partially reduced in the starting catalysts since no band attributable to carbonyls adsorbed on Cu^{2+} species, expected to yield bands of weakly held carbonyls above 2160 cm^{-1}, typically observable only at low temperatures or high equilibrium pressures [57], is detected. However, the possibility that the catalyst starts from a partially reduced state in the copper oxide component has been discarded on the basis of previous XPS and XANES characterization [8,9], as mentioned above and is further examined below. Alternatively, CO can also chemisorb on the ceria component giving rise to carbonate species (in which case, associated formal ceria reduction is produced) when it exposes metastable surfaces like the (1 1 0), while it would only physisorb over most stable (1 1 1) faces [59]. However, the amount of carbonate species formed upon room temperature interaction of CO with the copper-free supports is practically null [35]. On the other hand, the possibility that reduction of the catalyst can occur upon CO interaction at room temperature within a process basically involving interfacial copper oxide and ceria support sites has been evidenced by EPR and XPS in previous works [9,12,17,49]; indeed, about 70% of the copper has been

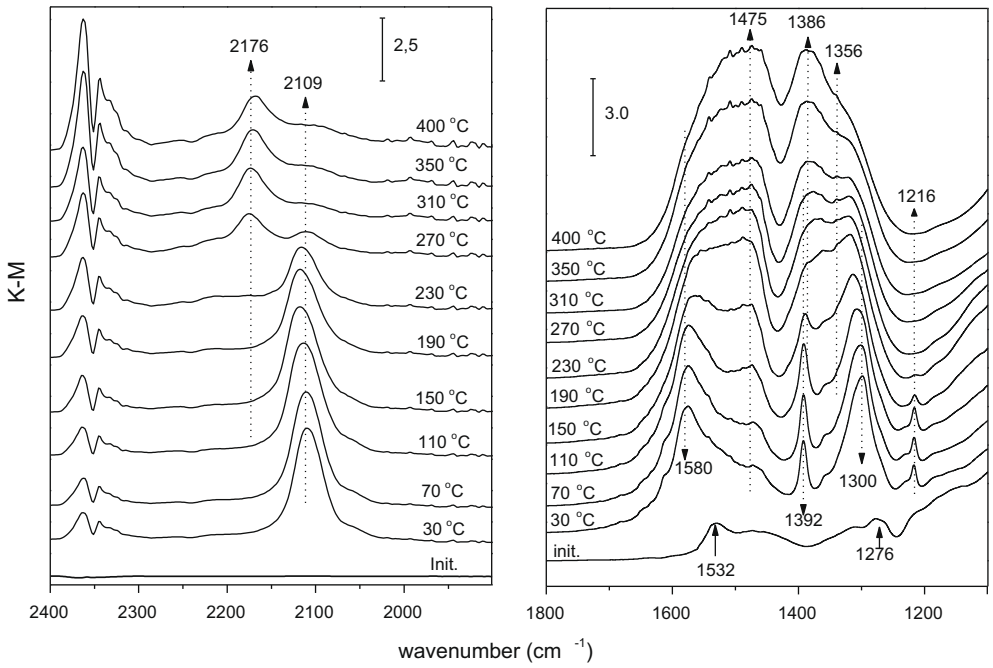

Fig. 4. DRIFTS spectra recorded at the indicated temperatures during the CO-TPR run over CuCe.

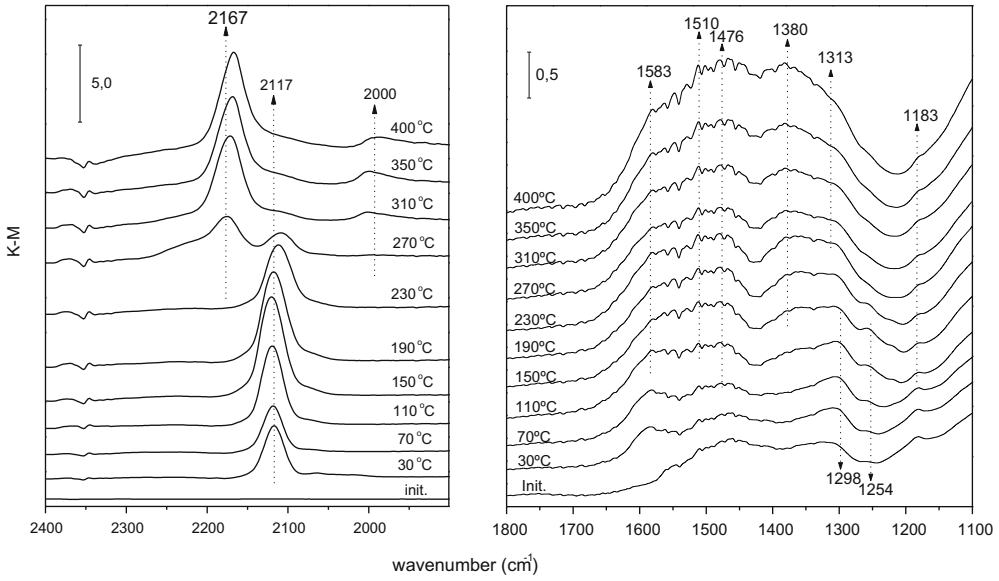

Fig. 5. DRIFTS spectra recorded at the indicated temperatures during the CO-TPR run over CuCeTb4.

estimated to become reduced to Cu^+ species upon CO interaction at room temperature with the CuCe catalyst [12]. A similar low temperature reduction process has also been proposed by Caputo et al. on the basis of CO-TPR experiments performed over catalysts of this type [36]. In this sense, the simultaneous formation of Cu^+-carbonyl and carbonate species in the copper-containing samples evidences the existence of a redox process by which CO_2 can be formed as a consequence of the copper oxide reduction process and subsequently chemisorbed in the form of carbonates over the ceria support (formally speaking: $2Cu^{2+} + 2O^{2-} + CO \rightarrow 2Cu^{+} + CO_3^{2-}$). Indeed, a correlation between the amounts of Cu^+-carbonyls and carbonate-type species formed at room temperature among the examined catalysts can be noted which gives further support to this hypothesis (Figs. 4–6). Furthermore, the magnitude of this low temperature reduction process also correlates with the CO oxidation activities observed under CO-PROX conditions over these samples [7,8]. It appears then that the degree of support promotion of the reduction of dispersed copper oxide entities to Cu^+ states during such low-temperature redox process, rather than redox processes occurring at higher temperature, which is the information typically provided by classical TPR tests like those shown in Figs. 1 and 3, is most relevant to explain the CO oxidation activities in this type of catalysts.

Concerning the analysis of correlations between evolution of Cu^+-carbonyl intensity and copper oxide reduction during the CO-TPR tests (Figs. 3 and 7), important differences are apparent as a function of the presence of terbium in the catalysts. It must be considered in this sense that Cu^+-carbonyls usually show signif-

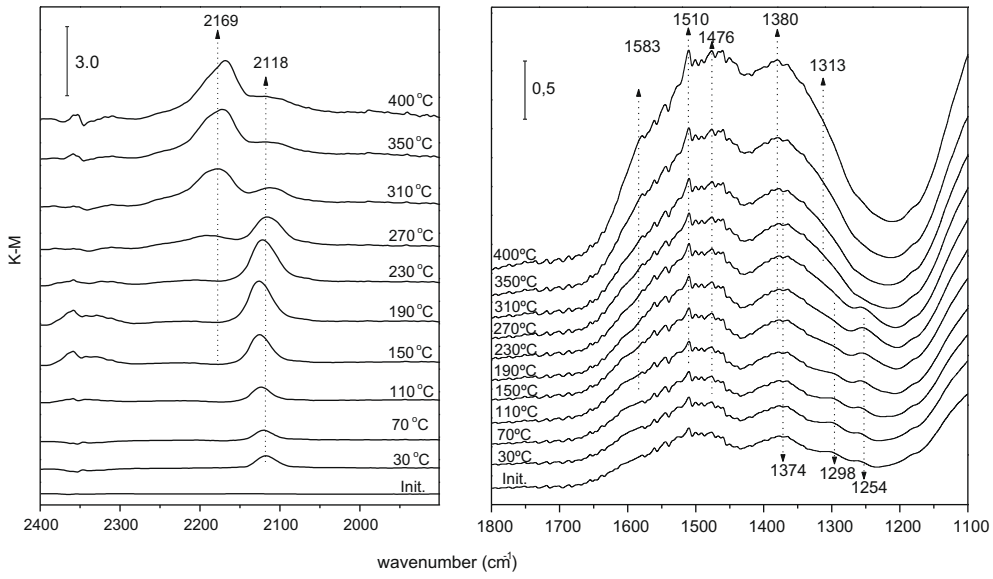

Fig. 6. DRIFTS spectra recorded at the indicated temperatures during the CO-TPR run over CuCeTb1.

Table 2
Spectral characteristics and proposed assignment of main CO-derived bands detected by DRIFTS in the course of CO-TPR tests over CuCe, CuCeTb4 and CuCeTb1 catalysts.

Species assignment[a]	Frequencies observed (cm^{-1}) and mode assignment
Bidentate carbonate	$\nu_{C=O}$: 1583–1580; $\nu_{O-C-O(asym)}$: 1313–1300
Mono- or poly-dentate carbonate[b]	$\nu(CO_3^{2-})_{(asym)}$: 1476–1475; $\nu(CO_3^{2-})_{(sym)}$: 1356
Hydrogen-carbonate	$\nu_{O-C-O(asym)}$: ≈ 1600; $\nu_{O-C-O(sym)}$: 1392 (1360); δ_{O-H}: 1216 (1216); ν_{O-H}: 3620 (3620)
Formate	$\nu_{O-C-O(asym)} + \delta_{C-H}$: ≈ 2940[c]; ν_{C-H}: 2845[d]. $\nu_{O-C-O(asym)}$: 1558–1590, $\nu_{O-C-O(sym)}$ 1330–1370
Carboxylate	$\nu_{O-C-O(asym)}$: 1510; $\nu_{O-C-O(sym)}$: 1390–1380
Ce^{4+}-carbonyl	ν_{CO}: 2176–2160
Cu^{+}-carbonyl	ν_{CO}: 2123–2009

[a] Assignment based on earlier reports in which further details can be found [52–55], and as also recently confirmed by isotopic shifts detected upon comparison of experiments of interaction of ^{12}CO and ^{13}CO with the CuCe sample [35].
[b] Similarities between frequencies do not allow a more definitive attribution; discussion on this can be found elsewhere [52].
[c] Mode assignment as proposed elsewhere [35]; however, $\nu_{O-C-O(asym)} + \nu_{O-C-O(sym)}$ combination, as proposed for formate species chemisorbed on zirconia [35], cannot be discarded, considering that the position of the $\nu_{O-C-O(asym)}$ vibration could not be fully resolved.
[d] The $\nu_{O-C-O(sym)}$ mode is expected to be the most intense vibration in this zone although the δ_{C-H} vibration could strongly overlap [35,54].

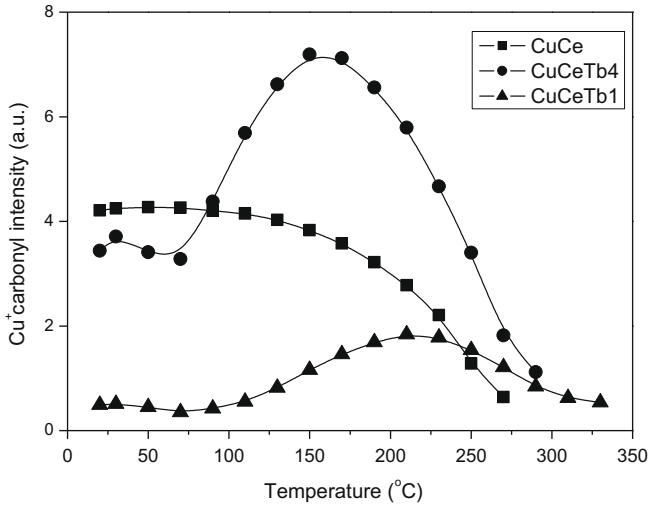

Fig. 7. Evolution of the intensity of the Cu^{+}-carbonyl species during the CO-TPR tests over the indicated samples.

icantly higher thermal stability than Cu^0 or Cu^{2+} carbonyls [60], the latter two not being expected to be stable under the employed conditions [35]. Thus, the decrease in Cu^{+}-carbonyl intensity detected with increasing temperature in CuCe suggests that full reduction of the dispersed CuO entities to metallic copper could be most favoured in this catalyst. In contrast, observation of a maximum in the Tb-containing samples (Fig. 7) suggests that a more gradual, sequential, copper reduction is produced in such cases, as also detected previously for zirconia-supported copper catalysts [61]. Thus, for CuCeTb4, the Cu^{+}-carbonyl intensity displays a maximum at 150 °C suggesting that reduction of Cu^{2+} to Cu^{+} is favoured up to that temperature while Cu^{+} reduction to metallic copper would be favoured at higher temperature. In turn, reduction of Cu^{2+} to Cu^{+} would be produced up to 210 °C over CuCeTb1 and subsequent reduction to copper metal would occur above this temperature. The different behaviour as a function of Tb presence in the support can be also related to the presence of electron transfer processes involving copper entities and terbium cations (i.e. $Cu^0 + Tb^{4+} \rightarrow Cu^{+} + Tb^{3+}$), which could comparatively be most favoured as a consequence of the higher stability of Tb^{3+} with respect to Ce^{3+} (not only for the free cations in solution but also within the fluorite oxide network [62]). However, we cannot discard that carbonyl evolutions displayed in Fig. 7 could be to some extent affected by a higher stability of the Cu^{+}-carbonyl in the presence of Tb in the support (according to the small red shift detected, as mentioned above). In this sense, XPS results point towards a higher difficulty for copper reduction in the presence of terbium, suggesting that the mentioned electron transfer processes could operate for the

$Ce_{1-x}Tb_xO_{2-y}$-supported systems, leading to a favoured stabilization of the partially reduced state of copper in the presence of terbium. Thus, as displayed in Fig. 8, the analysis of XPS results by means of Wagner chemical state plots (combining photoelectron and X-ray excited Auger lines [63,64]) indicates that copper appears as a fully oxidized Cu^{2+} in the initial CuCe and CuCeTb1 samples (in consistency also with the ratio observed between principal and satellite peaks in the Cu2p zone) although the shift of Cu(2p and AES) parameters with respect to those of pure CuO indicates some modifications of its electronic properties which must be related to the size of the particles and their interaction with the support [12]. Wagner's chemical state plot for the initial samples in Fig. 8 shows that copper parameters of CuCe fit on the dashed line of slope-3 of bulk CuO, which indicates that this is also the chemical state of the copper in this sample; however, the shift, along this line, from the bulk CuO parameters towards those found for CuO overloaded ZSM-5 zeolites [65] indicates a strong interaction of thin CuO-like small clusters with the ceria [12]. Noteworthy, this copper is almost completely reduced in CuCe to a Cu_2O-like phase after 30 min contact with 1 Torr of CO at 100 °C (see the shift towards the slope-3 dashed line of bulk Cu_2O in the diagram); in turn, about 84.6% of Ce^{4+} is inferred from factor analysis of the Ce3d zone (not shown) in the spectrum of this sample after such reduction treatment (while the starting sample showed a fully oxidized state for cerium). In the case of CuCeTb1, the starting sample treated only under O_2 at 200 °C displays Cu(2p and AES) parameters which suggest that copper (even though fully oxidized) could present a $Cu(OH)_2$–CuO mixed state. CuO-type state, similar to the starting one in CuCe, could however be achieved by thermal treatment under a stoichiometric CO–O_2 mixture up to 400 °C. When such sample is subjected to the same reduction treatment as CuCe (i.e. under 1 Torr of CO at 100 °C for 30 min), an appreciably lower degree of copper reduction is attained. However, terbium becomes appreciably reduced after such reduction treatment (from ca. 43% to ca. 72% of Tb^{3+}) while cerium becomes only residually reduced by such treatment (ca. 98% of Ce^{4+}). These results suggest the existence of electron transfer phenomena not only, as mentioned above, between copper and the support but also between cerium and terbium in the $Ce_{1-x}Tb_xO_{2-y}$-supported systems. In turn, the significant levels of support reduction achieved in any case after treatments under CO indicate that joint copper and support redox changes must be considered for full interpretation of CO-TPR profiles in this type of systems.

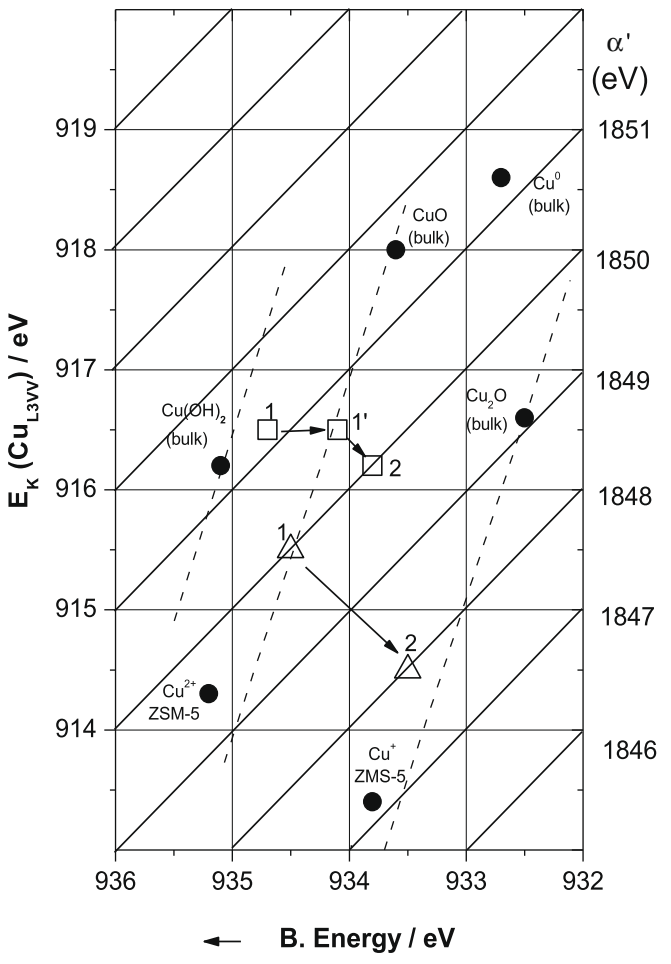

Fig. 8. Wagner diagrams showing the evolution of Cu (2p and AES) XP parameters during redox treatments performed over CuCe (triangles) and CuCeTb1 (squares). Treatments are indicated as 1 for the initial sample treated under O_2 at 200 °C and outgassed at the same temperature and 2 for the sample treated under CO at 100 °C. Intermediate treatment 1′ performed for the CuCeTb1 sample was done under stoichiometric CO–O_2 mixture at 400 °C.

4. Conclusions

The present work analyses in parallel results of *in situ* CO-TPR-DRIFTS-MS and CO-TPR-MS in a classical tubular reactor over catalysts with the same amount of copper oxide supported on pure ceria and $Ce_{1-x}Tb_xO_{2-y}$ mixed oxides. As typically done during classical TPR tests, the profiles are obtained after a period in which the reactant gas concentration becomes constant at the reactor outlet at room temperature after which the heating ramp is launched. According to the available literature, redox/catalytic correlations can be established on the basis of such TPR tests (done with either CO or, in most cases, H_2) in the sense that most active (for CO oxidation) well-dispersed copper oxide entities are reduced first while higher temperature is required for reduction of larger copper oxide crystals. Even though this general correlation can still be valid when the nature of the support is not changed, the results obtained here indicate that it cannot be applied in a general sense. Indeed, so-obtained CO-TPR results suggest that the reducibility of the catalyst increases by increasing the terbium content of the support, just opposite to CO oxidation activity obtained under CO-PROX conditions. The reason for the discrepancy is that main redox phenomena of relevancy for that reaction can apparently take place in the presence of CO already at room temperature, usually during gas equilibration period prior to launching the TPR heating ramp. Thus, the catalytic activity can be rather correlated to the level of CO consumed at room temperature or to the intensity of a particular Cu^+-carbonyl species formed upon such low temperature reduction process. In turn, significant degree of support reduction is detected upon interaction with CO in any case, as revealed also by XPS, which makes a complete interpretation of features obtained in the TPR profiles difficult. In turn, analysis of the evolution of Cu^+-carbonyls during the course of the TPR runs suggests the existence of electron transfer processes which could stabilize Cu^+ in the presence of terbium. This is in agreement with a higher difficulty for copper reduction in the presence of terbium, according to XPS investigation which also reveals a higher stability of fully oxidized state of cerium most likely due to favoured electron transfer phenomena between cerium and terbium in the fluorite lattice.

Acknowledgements

A.H. and A.L.C. thank the MEC and CSIC for FPU and JAE PhD grants-contracts, respectively, under which their contribution to this work was done. P.B. is thankful to 6th European Community Framework Program for a Marie Curie Incoming International

Fellowship. The authors also thank the MEC or MICINN (projects CTQ2006-15600/BQU and CTQ2009-14527) and Comunidad de Madrid (project ENERCAM S-0505/ENE/000304) for financial support.

References

[1] G. Jacobs, L. Williams, U. Graham, D. Sparks, B.H. Davis, J. Phys. Chem. B 107 (2003) 10398.
[2] A. Martínez-Arias, M. Fernández-García, A.B. Hungría, A. Iglesias-Juez, O. Gálvez, J.A. Anderson, J.C. Conesa, J. Soria, G. Munuera, J. Catal. 214 (2003) 261.
[3] P. Bera, S. Malwadkar, A. Gayen, C.V.V. Satyanarayana, B.S. Rao, M.S. Hegde, Catal. Lett. 96 (2004) 213.
[4] X. Wang, J.A. Rodríguez, J.C. Hanson, D. Gamarra, A. Martínez-Arias, M. Fernández-García, J. Phys. Chem. B 110 (2006) 428.
[5] P. Ratnasamy, D. Srinivas, C.V.V. Satyanarayana, P. Manikandan, R.S.S. Kumaran, M. Sachin, V.N. Shetti, J. Catal. 221 (2004) 455.
[6] A. Martínez-Arias, A.B. Hungría, G. Munuera, D. Gamarra, Appl. Catal. B 65 (2006) 207.
[7] D. Gamarra, C. Belver, M. Fernández-García, A. Martínez-Arias, J. Am. Chem. Soc. 129 (2007) 12064.
[8] A. Martínez-Arias, A.B. Hungría, M. Fernández-García, J.C. Conesa, G. Munuera, J. Power Sources 151 (2005) 32.
[9] D. Gamarra, G. Munuera, A.B. Hungría, M. Fernández-García, J.C. Conesa, P.A. Midgley, X.Q. Wang, J.C. Hanson, J.A. Rodríguez, A. Martínez-Arias, J. Phys. Chem. C 111 (2007) 11026.
[10] G. Avgouropoulos, T. Ioannides, Ch. Papadopoulou, J. Batista, S. Hocevar, H.K. Matralis, Catal. Today 75 (2002) 157.
[11] G. Sedmak, S. Hocevar, J. Levec, J. Catal. 213 (2003) 135.
[12] A. Martínez-Arias, A.B. Hungría, M. Fernández-García, J.C. Conesa, G. Munuera, J. Phys. Chem. B 108 (2004) 17983.
[13] W. Liu, A.F. Sarofim, M. Flytzani-Stephanopoulos, Chem. Eng. Sci. 49 (1995) 4871.
[14] H.C. Lee, D.H. Kim, Catal. Today 132 (2008) 109.
[15] N. Bion, F. Epron, M. Moreno, F. Mariño, D. Duprez, Top. Catal. 51 (2008) 76.
[16] I. López, T. Valdés-Solís, G. Marbán, Int. J. Hydrogen Energ. 33 (2008) 197.
[17] A. Martínez-Arias, M. Fernández-García, O. Gálvez, J.M. Coronado, J.A. Anderson, J.C. Conesa, J. Soria, G. Munuera, J. Catal. 195 (2000) 207.
[18] M.-F. Luo, Y.-P. Song, J.-Q. Lu, X.-Y. Wang, Z.-Y. Pu, J. Phys. Chem. C 111 (2007) 12686.
[19] X. Wang, J.A. Rodriguez, J.C. Hanson, D. Gamarra, A. Martínez-Arias, M. Fernández-García, J. Phys. Chem. B 109 (2005) 19595.
[20] A. Martínez-Arias, M. Fernández-García, V. Ballesteros, L.N. Salamanca, J.C. Conesa, C. Otero, J. Soria, Langmuir 15 (1999) 4796.
[21] A.B. Hungría, A. Martínez-Arias, M. Fernández-García, A. Iglesias-Juez, A. Guerrero-Ruiz, J.J. Calvino, J.C. Conesa, J. Soria, Chem. Mater. 15 (2003) 4309.
[22] J.P. Holgado, R. Alvarez, G. Munuera, Appl. Surf. Sci. 161 (2000) 164.
[23] A. Martínez-Arias, A.B. Hungría, M. Fernández-García, A. Iglesias-Juez, J.C. Conesa, G.C. Mather, G. Munuera, J. Power Sources 151 (2005) 43.
[24] P. Shuk, M. Greenblatt, M. Croft, Chem. Mater. 11 (1999) 473.
[25] X.Q. Wang, J.C. Hanson, A.I. Frenkel, J.-Y. Kim, J.A. Rodriguez, J. Phys. Chem. B 108 (2004) 13667.
[26] J.B. Wang, S.-C. Lin, T.-J. Huang, Appl. Catal. A 232 (2002) 107.
[27] M. Fernández-García, A. Martínez-Arias, J.C. Hanson, J.A. Rodriguez, Chem. Rev. 104 (2004) 4063.
[28] R.-X. Zhou, T.-M. Yu, X.-Y. Jiang, F. Chen, X.-M. Zheng, Appl. Surf. Sci. 148 (1999) 263.
[29] J. Papavasiliou, G. Avogouropoulos, T. Ioannides, Catal. Commun. 5 (2004) 231.
[30] A. Pintar, J. Batista, S. Hocevar, J. Colloid Interf. Sci. 285 (2005) 218.
[31] M.-F. Luo, J.-M. Ma, J.-Q. Lu, Y.-P. Song, Y.-J. Wang, J. Catal. 246 (2007) 52.
[32] D. Gamarra, A. Hornés, Zs. Koppány, Z. Schay, G. Munuera, J. Soria, A. Martínez-Arias, J. Power Sources 169 (2007) 110.
[33] K. Jagannathan, A. Srinivasan, M.S. Hedge, C.N.R. Rao, Surf. Sci. 99 (1980) 309.
[34] A. Martínez-Arias, R. Cataluña, J.C. Conesa, J. Soria, J. Phys. Chem. B 102 (1998) 809.
[35] P. Bera, A. López Cámara, A. Hornés, A. Martínez-Arias, J. Phys. Chem. C 113 (2009) 10689.
[36] T. Caputo, L. Lisi, R. Pirone, G. Russo, Appl. Catal. A 348 (2008) 42.
[37] (a) C. Padeste, N.W. Cant, D.L. Trimm, Catal. Lett. 18 (1993) 305;
A. Badri, J. Lamotte, J.C. Lavalley, A. Laachir, V. Perrichon, O. Touret, G.N. Sauvion, E. Quemere, Eur. J. Solid State Inorg. Chem. 28 (1991) 445.
[38] Q. Liang, X. Wu, D. Weng, Z. Lu, Catal. Commun. 9 (2008) 202.
[39] X. Wang, J.C. Hanson, G. Liu, J.A. Rodríguez, A. Iglesias-Juez, M. Fernández-García, J. Chem. Phys. 121 (2004) 5434.
[40] P. Bera, K.R. Priolkar, P.R. Sarode, M.S. Hegde, S. Emura, R. Kumashiro, N.P. Lalla, Chem. Mater. 14 (2002) 3591.
[41] W. Shan, W. Shen, C. Li, Chem. Mater. 15 (2003) 4761.
[42] G.R. Rao, H.R. Sahu, B.G. Mishra, Colloid. Surf. A 220 (2003) 261.
[43] H. Zou, X. Dong, W. Lin, Appl. Surf. Sci. 253 (2006) 2893.
[44] A.A. Firsova, A.N. Ilichev, T.I. Khomenko, L.V. Gorobinskii, Y.V. Maksimov, I.P. Suzdalev, V.N. Korchak, Kinet. Catal. 48 (2007) 282.
[45] J.B. Wang, W.-H. Shih, T.-J. Huang, Appl. Catal. A 203 (2000) 191.
[46] J.B. Wang, D.-H. Tsai, T.-J. Huang, J. Catal. 208 (2002) 370.
[47] T. Caputo, R. Pirone, G. Russo, Kinet. Catal. 47 (2006) 756.
[48] M.-F. Luo, X.-M. Cheng, Acta Chem. Scand. 52 (1998) 1183.
[49] A. Martínez-Arias, M. Fernández-García, J. Soria, J.C. Conesa, J. Catal. 182 (1999) 367.
[50] A. Martínez-Arias, D. Gamarra, M. Fernández-García, X.Q. Wang, J.C. Hanson, J.A. Rodriguez, J. Catal. 240 (2006) 1.
[51] C.S. Polster, H. Nair, C.D. Baertsch, J. Catal. 266 (2009) 308.
[52] C. Binet, M. Daturi, J.-C. Lavalley, Catal. Today 50 (1999) 207.
[53] C. Li, Y. Sakata, T. Arai, K. Domen, K.-I. Maruya, T. Onishi, J. Chem. Soc. Faraday Trans. 1 (85) (1989) 929.
[54] C. Li, Y. Sakata, T. Arai, K. Domen, K.-I. Maruya, T. Onishi, J. Chem. Soc. Faraday Trans. 1 (85) (1989) 1451.
[55] K.I. Hadjiivanov, G.N. Vayssilov, Adv. Catal. 47 (2002) 307.
[56] A. Trovarelli (Ed.), Catalysis by Ceria and Related Materials, Imperial College Press, London, 2002.
[57] K.I. Hadjiivanov, M. Kantcheva, D.G. Klissurski, J. Chem. Soc. Faraday Trans. 92 (1996) 4595.
[58] D. Scarano, S. Bordiga, C. Lamberti, G. Spoto, G. Ricchiardi, A. Zecchina, C. Otero Areán, Surf. Sci. 411 (1998) 272.
[59] M. Huang, S. Fabris, J. Phys. Chem. C 112 (2008) 8643.
[60] M.B. Padley, C.H. Rochester, G.J. Hutchings, F. King, J. Catal. 148 (1994) 438.
[61] V. Indovina, M. Occhiuzzi, D. Pietrogiacomi, S. Tuti, J. Phys. Chem. B 103 (1999) 9967.
[62] L.P. Li, Q. Wei, H.J. Liu, D.F. Zheng, W.H. Su, Z. Phys. Condens. Mater. 96 (1995) 451.
[63] C.D. Wagner, Faraday Discuss. Chem. Soc. 60 (1975) 291.
[64] G. Moretti, J. Electron Spectrosc. Relat. Phenom. 95 (1998) 95.
[65] W. Grünert, N.W. Hayes, R.W. Joyner, E.S. Shpiro, J. Phys. Chem. 98 (1994) 10832.